Astrophysical Masers and their Environments
Proceedings IAU Symposium No. 242, 2007
J.M. Chapman & W.A. Baan, eds.

doi:10.1017/S1743921307013117

SiO maser observations of a wide dust-temperature range sample

Jun-ichi Nakashima[1] and Shuji Deguchi[2]

[1]Academia Sinica Institute of Astronomy and Astrophysics, P.O. Box 23-141, Taipei 10617, Taiwan
email: junichi@asiaa.sinica.edu.tw

[2]Nobeyama Radio Observatory, National Astronomical Observatory, Minamimaki, Minamisaku, Nagano 384-1305, Japan

Abstract. We present the results of SiO line observations of a sample of known SiO maser sources covering a wide dust-temperature range. The aim of the present research is to investigate the causes of the correlation between infrared colors and SiO maser intensity ratios among different transition lines. We observed in total 75 SiO maser sources with the Nobeyama 45m telescope quasi-simultaneously in the SiO $J = 1{-}0$ $v = 0$, 1, 2, 3, 4 and $J = 2{-}1$ $v = 1$, 2 lines. We also observed the sample in the ^{29}SiO $J = 1{-}0$ $v = 0$ and $J = 2{-}1$ $v = 0$, and ^{30}SiO $J = 1{-}0$ $v = 0$ lines, and the H_2O $6_{1,6}{-}5_{2,3}$ line. As reported in previous papers, we confirmed that the intensity ratios of the SiO $J = 1{-}0$ $v = 2$ to $v = 1$ lines clearly correlate with infrared colors. In addition, we found possible correlation between infrared colors and the intensity ratios of the SiO $J = 1{-}0$ $v = 3$ to $v = 1\&2$ lines.

Keywords. masers — stars: AGB and post-AGB — stars: late-type — stars: mass loss — stars: statistics

1. Introduction

An important problem in the studies of SiO masers was that the sample of all known SiO maser sources was considerably biased. Specifically, the dust (effective) temperature of known SiO maser sources, which was calculated from mid-infrared flux densities (such as the IRAS and MSX flux densities), was limited roughly to the range of 250 K $\lesssim T_{\rm dust} \lesssim$ 2000 K. This is because the previous SiO maser surveys have been limited to relatively warm dust-temperature ranges. Consequently a non-negligible number of potential SiO maser sources (especially with a low dust-temperature) have been omitted from the previous SiO maser surveys.

Nyman *et al.* (1993) first realized the importance of SiO maser sources exhibiting a low dust-temperature. They investigated how SiO maser emission behaves in a low dust-temperature range by observing OH/IR stars in the SiO $J = 1{-}0$ $v = 1\&2$ and $J = 2{-}1$ $v = 1$ lines. The OH/IR stars often exhibit a low dust-temperature less than $T_{\rm dust} = 250$ K. In their observations the cold objects clearly show a larger intensity ratio of the SiO $J = 1{-}0$ $v = 2$ to $v = 1$ lines. Both collisional and radiative schemes cannot fully explain this observational property of the SiO masers (Bujarrabal 1994; Doel *et al.* 1995). Nyman *et al.* (1993) suggested that an infrared H_2O line ($11_{6,6}$ $\nu_2 = 1 \rightarrow 12_{7,5}$ $\nu_2 = 0$) overlapping with the SiO $J = 0$ $v = 1 \rightarrow J = 1$ $v = 2$ transition might play an important role. However, in the early 1990s the number of cold SiO maser sources (like OH/IR stars) was quite limited, and it was difficult to statistically investigate the relation between infrared colors and the intensity ratios of SiO maser lines.

Nakashima & Deguchi (2003b) recently extended the Nyman *et al.* (1993) study by surveying SiO maser emissions in cold, dusty IRAS sources exhibiting dust temperature

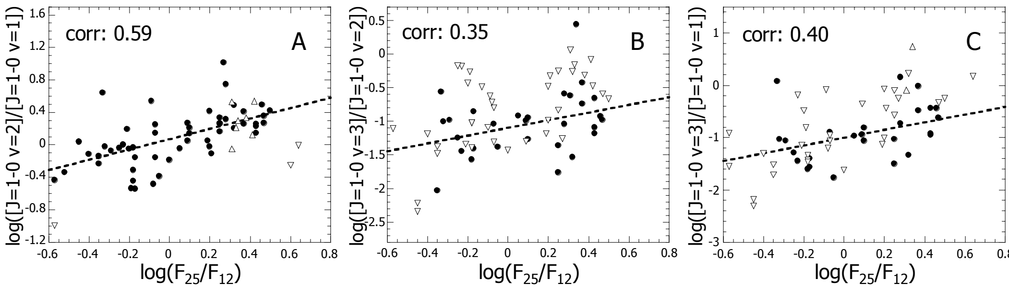

Figure 1. Infrared colors versus intensity ratio of SiO maser lines. The horizontal axes represent infrared colors. F_{25} and F_{12} denote the IRAS flux densities at $\lambda = 25$ and 12 μm, respectively. The filled dots (•), upward triangles (△) and downward triangles (▽) respectively represent the intensity ratios of the SiO maser lines, lower limits of the ratio and upper limits of the ratio. Correlation coefficients are given in the upper-left corners of each panel. The dashed lines are the results of least-square fitting of a first order polynomial.

less than 250 K. They found roughly 40 new SiO maser sources in the cold dusty objects and, in conjunction with the results of another SiO maser survey of relatively warm IRAS objects (Nakashima & Deguchi 2003a), they clearly demonstrated that the intensity ratio of the SiO $J = 1{-}0$ $v = 2$ to $v = 1$ lines increases inversely proportional to the dust temperature. Nakashima & Deguchi (2003b) again suggested that the line overlap with H_2O might explain this correlation if the line overlap becomes stronger with decreasing dust temperature. To further consider this problem, we need to confirm whether properties of the SiO lines other than the $J = 1{-}0$ $v = 1$ and 2 lines are consistent with the existence of H_2O line overlap. In this contributed paper, we present the result of quasi-simultaneous observations in the multiple different SiO rotational lines with the Nobeyama 45m telescope. The main aim of the observation is to check the behavior of SiO maser intensity ratios including lines other than the $J = 1{-}0$ $v = 1$ and 2 lines.

2. Observations and results

The observing targets were selected from Nakashima & Deguchi(2003a, b) and the Nobeyama SiO maser source catalog (Gorny *et al.* in preparation) in terms of the IRAS colors and flux densities. The targets are distributed roughly in the right ascension range between $18^{\rm h}$ and $22^{\rm h}$, because the cold SiO maser sources found by Nakashima & Deguchi (2003b) are distributed roughly in this range. We selected the observing targets basically in order of the brightness at $\lambda = 12$ μm, but we also paid attention to the source distribution in the IRAS two-color diagram so that the observing targets continuously cover the entire color range.

SiO line observations with the Nobeyama 45m telescope were made in two separated periods: May 11–19, 2004 and February 15–19, 2006. In the first period we observed a total of 38 objects. The observed SiO transitions in the first period were $J = 1{-}0$ $v = 1, 2, 3$ and $J = 2{-}1$ $v = 1, 2$. We also observed the ^{29}SiO $J = 1{-}0$ $v = 0$ and $J = 2{-}1$ $v = 0$ lines. In addition, we observed 27 objects in the H_2O maser line at 22 GHz $(6_{1,6}-5_{2,3})$ as a backup observation under rainy/heavy cloud conditions. In the second period we observed, in total, 53 objects. The observed transitions in the second period were SiO $J = 1{-}0$ $v = 0, 1, 2, 3, 4$, ^{29}SiO $J = 1{-}0$ $v = 0$ and ^{30}SiO $J = 1{-}0$ $v = 0$. The technical details of the observations will be presented in our future paper (Nakashima & Deguchi, in preparation).

https://doi.org/10.1017/S1743921307013117 Published online by Cambridge University Press

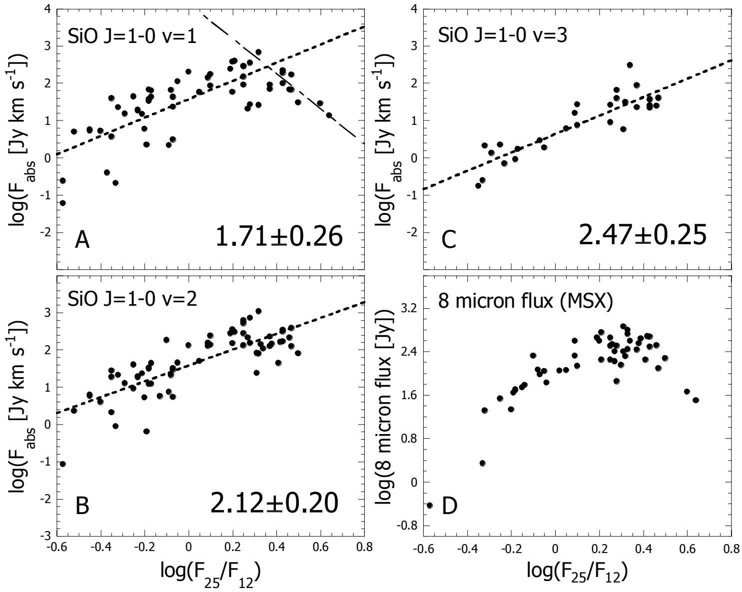

Figure 2. [*Panels A, B and C*]: Relation between infrared colors and absolute intensity of SiO maser lines. The notation of the infrared colors is same with that used in Figure 1. The intensity of SiO maser lines is standardized at the distance of 1 kpc. The thick dashed lines represent the results of least-square-fitting of a first order polynomial. The inclinations of the fitted lines (thick dashed lines) are given at the lower-right corners of each panel with statistical uncertainty. In the panel A, only the data points below $\log(F_{25}/F_{12}) = 0.5$ were fitted by the polynomial. The data points above $\log(F_{25}/F_{12}) = 0.5$ are independently fitted by a first order polynomial, and the results of the fitting is given as the chain line. [*Panel D*]: Relation between 8μm absolute flux density and infrared color. The 8μm flux is standardized at the distance of 1 kpc.

In this paper, we focus on the properties of the SiO $J = 1\text{–}0$ $v = 1$, 2 and 3 lines, in which we detected a large number of objects for statistical analysis. Figure 1 shows the relation between infrared colors and intensity ratios among the SiO maser lines. The line intensities used to calculate the intensity ratios are velocity-integrated intensities. In panel A of Figure 1 we can clearly confirm the positive correlation between the $\log(F_{25}/F_{12})$ color and the intensity ratio of the SiO $J = 1\text{–}0$ $v = 2$ to $v = 1$ lines as reported by Nakashima & Deguchi (2003b). Interestingly, the intensity ratios of the $J = 1\text{–}0$ $v = 3$ to $v = 2$ lines and of the $J = 1\text{–}0$ $v = 3$ to $v = 1$ lines seem to also correlate with the $\log(F_{25}/F_{12})$ color (see, panels B and C) even though the correlation coefficients are slightly smaller than that of panel A.

Figure 2 shows the relations between infrared colors and absolute intensities of the SiO maser lines. The intensity of the SiO maser lines is standardized at the distance of 1 kpc using the luminosity distances. The panels A, B and C of Figure 2 show the relations between the $\log(F_{25}/F_{12})$ color and the absolute intensity of the SiO $J = 1\text{–}0$ $v = 1$, 2 and 3 lines. A notable feature seen in these panels is that the SiO maser absolute intensities undoubtedly correlate with the $\log(F_{25}/F_{12})$ color. Another clear feature is that for higher vibrational transitions, the dashed lines representing the least-square-fitting with a first-order polynomial also become steeper. This tendency is consistent with the correlation seen in Figure 1. In panel A in Figure 2, the values of the absolute intensity of the SiO maser emission seem to maximize at $\log(F_{25}/F_{12}) \sim 0.5$, and the values tend to decrease with increasing color in the red region above $\log(F_{25}/F_{12}) = 0.5$. The $\log(F_{25}/F_{12})$ color of 0.5 corresponds to the boundary between distributions of

https://doi.org/10.1017/S1743921307013117 Published online by Cambridge University Press

AGB and post-AGB stars in the $\log(F_{25}/F_{12})$ color. In fact, panel A in Figure 1 (and Figure 8 in Nakashima & Deguchi 2003b) shows a sudden change in strength of the feature at $\log(F_{25}/F_{12}) \sim 0.5$. No such change is seen in the panels B and C in Figure 2, simply because the SiO $J = 1\text{–}0$ $v = 2$ and 3 lines have not been detected above $\log(F_{25}/F_{12}) = 0.5$ in the present observations.

A possible reason for the correlation seen in panels A, B and C in Figure 2 is that the energy input to the SiO maser region increases with the infrared colors. To confirm this possibility, in panel D in Figure 2 we plotted the 8μm flux densities as a function of the infrared colors. The values of the 8μm flux densities were taken from the MSX point source catalog. If we rely on the radiative scheme the 8μm flux should well represent the energy input to the SiO maser region, because the $\lambda = 8\mu$m corresponds to the $\Delta v = 1$ SiO transition (e.g., Deguchi & Iguchi 1976). In panel D in Figure 2, the 8μm flux densities are standardized to the distance of 1kpc using the luminosity distance. The distribution of the data points seen in panel D is, in fact, strikingly similar with those seen in panels A, B and C, supporting the idea that the 8μm flux tightly correlates with the SiO maser intensity as suggested by Bujarrabal *et al.* (1987).

3. Discussion

In this section we discuss the possible explanation for the correlation between infrared colors and SiO maser intensity ratios among the $v = 1$, 2 and 3 lines at 43 GHz. One possible explanation is to introduce the line overlap with H_2O ($11_{6,6}$ $\nu_2 = 1 \rightarrow 12_{7,5}$ $\nu_2 = 0$), which has been first suggested by Olofsson *et al.* (1981) to explain the anomalous, weak intensity of the SiO $J = 2\text{–}1$ $v = 2$ line in oxygen-rich (O-rich) stars. The H_2O line overlaps with the SiO $J = 0$ $v = 1 \rightarrow J = 1$ $v = 2$ transition with a velocity difference of 1 km s^{-1}. With this line overlap, the $J = 1$ $v = 2$ level is overpopulated, and the weakness of the SiO $J = 2\text{–}1$ $v = 2$ line is explained by this overpopulation. The overpopulation at the $J = 1$ $v = 2$ level is also consistent with the strong intensity of the $J = 1\text{–}0$ $v = 2$ line. Thus, the correlation between the infrared colors and the intensity ratio of the SiO $J = 1\text{–}0$ $v = 2$ to $v = 1$ lines may be explained if this line overlap with H_2O becomes stronger with increase of the infrared colors. One problem in this interpretation is that the intensity ratios of the SiO $J = 1\text{–}0$ $v = 3$ to $v = 1$&2 lines cannot be explained only with the H_2O $11_{6,6}$ $\nu_2 = 1 \rightarrow 12_{7,5}$ $\nu_2 = 0$ line. However Cho *et al.* (2007) recently reported an interesting detection of the SiO $J = 2\text{–}1$ $v = 3$ line toward an S-type star, χ Cyg. They also confirmed that the SiO $J = 2\text{–}1$ $v = 3$ line is weak in O-rich stars. The S-type stars have almost the same amount of oxygen and carbon atoms in their envelopes, and consequently they have few H_2O molecules in the envelopes. These results potentially suggest that another line overlap with H_2O affects the population distribution of SiO in O-rich stars, and Cho *et al.* (2007) have suggested that the H_2O $5_{0,5}$ $\nu_2 = 2 \rightarrow 6_{3,4}$ $\nu_2 = 1$ line overlapping with the SiO $J = 0$ $v = 2 \rightarrow J = 1$ $v = 3$ line (with a velocity difference of about 1.5 km s^{-1}) acts on the population distribution of SiO. Thus, if both H_2O $11_{6,6}$ $\nu_2 = 1 \rightarrow 12_{7,5}$ $\nu_2 = 0$ and $5_{0,5}$ $\nu_2 = 2 \rightarrow 6_{3,4}$ $\nu_2 = 1$ lines become stronger with increasing infrared colors, all correlations between infrared colors and the SiO maser intensity ratios among the $J = 1\text{–}0$ $v = 1$, 2 and 3 lines might be explained. The line intensity of the H_2O $5_{0,5}$ $\nu_2 = 2 \rightarrow 6_{3,4}$ $\nu_2 = 1$ line is usually weaker than that of the $11_{6,6}$ $\nu_2 = 1 \rightarrow 12_{7,5}$ $\nu_2 = 0$line. This fact also seems to be consistent with the relatively weak intensity of the SiO $J = 1\text{–}0$ $v = 3$ line.

However, there are some other problems with the explanation of the line overlap with H_2O. First, we have to explain how the H_2O infrared lines overlapping with the SiO lines become stronger with increasing infrared colors. The relative abundance of H_2O

https://doi.org/10.1017/S1743921307013117 Published online by Cambridge University Press

molecules possibly increases with infrared colors, but this is not conclusive. Second, the correlation between infrared colors and the intensity ratios of the SiO $J=1{-}0$ $v=2$ to $v=1$ lines might be explained without line overlap with H_2O. In the envelopes of very cold objects, strong 8μm emission comes from every direction to the SiO masering region, causing ineffective pumping through the SiO $\Delta v=1$ transition. On the other hand, 4μm emission corresponding to the SiO $\Delta v=2$ transition is more effectively pumping the SiO population instead of the 8μm emission. These processes might explain the correlation seen in Figure 2 (e.g., Doel *et al.* 1995). Third, a recent theoretical calculation predicted that if we introduce line overlap with H_2O, the spatial distribution of the maser spots cannot be theoretically reproduced (Soria-Ruiz *et al.* 2004). Thus, this problem will remain controversial for some more time.

4. Summary

In this research we observed 75 known SiO maser sources quasi-simultaneously in the SiO $J=1{-}0$, $v=0$, 1, 2, 3 and 4 lines, SiO $J=2{-}1$ $v=1$ and 2, ^{29}SiO $J=1{-}0$ $v=0$ and $J=2{-}1$ $v=0$, and ^{30}SiO $J=1{-}0$ $v=0$ lines. We also observed the targets in the H_2O $6_{1,6}{-}5_{2,3}$ line under rainy/heavy cloud condition. The sample continuously covers a very wide dust-temperature range from 150 K to 2000 K. The correlation between infrared colors and the intensity ratio of the SiO $J=1{-}0$ $v=2$ to $v=1$ lines is confirmed as reported by Nakashima & Deguchi (2003b). The intensity ratios of the SiO $J=1{-}0$ $v=3$ to $v=1$&2 lines possibly correlate with infrared colors. The line overlaps with H_2O might explain the correlations between the infrared colors and the SiO maser intensity ratios among the $J=1{-}0$ $v=1$, 2 and 3 lines, although there are alternative ways to interpret the phenomena.

Acknowledgements

The present research has been supported by the Academia Sinica Institute of Astronomy & Astrophysics in Taiwan.

References

Bujarrabal, V. 1994, *A&A* 285, 953
Bujarrabal, V., Planesas, P., & del Romero, A. 1987, *A&A* 175, 164
Cho, S.-H., Lee, C. W., & Park, Y.-S. 2007, *ApJ* 657, 482
Deguchi, S., & Iguchi, T. 1976, *PASJ* 28, 307
Doel, R. C., *et al.* 1995, *A&A* 302, 797
Nakashima, J., & Deguchi, S. 2003a, *PASJ* 55, 203
Nakashima, J., & Deguchi, S. 2003b, *PASJ* 55, 229
Nyman, L.-Å., Hall, P. J., & Le Bertre, T. 1993, *A&A* 280, 551
Olofsson, H., Rydbeck, O. E. H., Lane, A. P., & Predmore, C. R. 1981, *ApJ* 247, L81
Olofsson, H., Rydbeck, O. E. H., & Nyman, L.-A. *A&A* 150, 169
Soria-Ruiz, R., *et al.* 2004, *A&A* 426, 131